Journal of Marine Science and Technology

Volume 24 | Issue 4 Article 14

LOAD TRANSFER AND DEFORMATION ANALYSES OF PILED-RAFT FOUNDATION IN TAIPEI METROPOLITAN

Der-Guey Lin
Department of Soil and Water conservation, National Chung-Hsing University, Taichung, Taiwan, R.O.C

Wen-Tsung Liu
Department of Civil Engineering, Kao-Yuan University, Kaohsiung, Taiwan, R.O.C.

Jui-Ching Chou
Sinotech Engineering Consultants, Taipei, Taiwan, R.O.C., dglin@dragon.nchu.edu.tw

Recommended Citation

Lin, Der-Guey; Liu, Wen-Tsung; and Chou, Jui-Ching (2016) "LOAD TRANSFER AND DEFORMATION ANALYSES OF PILED-RAFT FOUNDATION IN TAIPEI METROPOLITAN," *Journal of Marine Science and Technology*: Vol. 24: Iss. 4, Article 14.
DOI: 10.6119/JMST-016-0315-1
Available at: https://jmstt.ntou.edu.tw/journal/vol24/iss4/14

Journal of Marine Science and Technology, Vol. 24, No. 4, pp. 798-806 (2016)
DOI: 10.6119/JMST-016-0315-1

LOAD TRANSFER AND DEFORMATION ANALYSES OF PILED-RAFT FOUNDATION IN TAIPEI METROPOLITAN

Der-Guey Lin[1], Wen-Tsung Liu[2], and Jui-Ching Chou[3]

Key words: piled-raft foundation, load-carrying ratio of the raft, FLAC 3D, settlement.

ABSTRACT

Piled-raft systems are often suitable for foundations of high-rise buildings to increase the bearing capacity and reduce the excessive settlement of foundations. However, the conventional design of the piled-raft foundation commonly ignores the bearing effect of the raft. A parametric study on the piled-raft foundation performance including the bearing effect for typical Taipei Subsoil is investigated using 3D FDM program, FLAC 3D. Input parameters of the parametric study are back calculated from a series of static pile loading tests implemented on the jobsite of TIFC (Taipei International Financial Corporation or *Taipei 101*). Parametric study results show that the load-carrying ratio of the raft depends on the number of piles of the pile group and the level of loading applied to the piled-raft foundation. This also shows that the raft of the piled-raft foundation is capable of sharing load. In addition, the settlement, differential settlement and bending moment of the piled-raft foundation are also discussed in this article.

I. INTRODUCTION

The possibility of using a piled-raft foundation to support superstructures as an economical alternative to the conventional piled foundation is gaining popularity in recent years. The design of piled-raft foundations requires analyses considering the load transferring mechanisms between pile, soil and raft (Poulos et al., 1997). Three types of analyses developed for the piled-raft foundation are commonly used: (1) simplified calculation methods – simplifications on modeling the pile, soil and raft interactions (Poulos and Davis, 1980; Randolph, 1983 and 1994); (2) approximate computer-based analyses – using strip on springs approach (Poulos, 1991) or plate on springs approach (Clancy and Randolph, 1993; Poulos, 1994); and (3) more rigorous computer-based methods - boundary element methods, 3-D FEM (Oh et al., 2009; Lee et al., 2010; Poulos et al., 2011; Karim et al., 2013; Nguyen et al., 2014) or 3-D FDM (Comodromos et al., 2009). In order to mimic the actual field conditions, 3-D FEM or 3-D FDM analyses are desirable. 3-D FEM usually requires a large amount of computer storage and time but 3-D FDM on the other hand is memory and simulation time efficient with practically acceptable accuracy. The present study chooses 3-D FDM (FLAC 3D) as the prime software for the analysis of the piled-raft foundation.

In the conventional design of the piled-raft foundation and the design practice in Taiwan, the contribution of load carrying by the raft is usually ignored. However, recent studies on real case histories and full scale pile group tests (Liang et al., 2003; Lee et al., 2010; Long, 2010) demonstrated that the raft can carry 15% to 70% of the total load.

The present study therefore attempts to assess the piled-raft foundation behavior and to broaden the understanding of the complex interaction between the piles, raft and soil via numerical simulations. First, pile load tests on the jobsite of TIFC (Taipei International Financial Corporation or *Taipei 101*) are modeled to calibrate input parameters of piles. Second, a parametric study is performed to study effects of the raft thickness, the number of piles and the loading level on the settlement, the bending moment and the load carrying ratio of the raft for a typical Taipei Metropolitan soil profile.

II. PILE LOADING TEST SIMULATION

As shown in Fig. 1, *Taipei 101* Construction Project (or *Taipei 101*) possesses a deep excavation at Tower Zone and Podium Zone with total excavation area of 152.20 m × 159.14 m × 21.7 m. A total of 508 bored piles were installed beneath the mat foundation of basement. In *Taipei 101*, five pile loading tests (three extension piles, P241, P335 and P532, and two compression piles, P39, P112) were performed. The testing piles

Paper submitted 08/17/15; revised 01/08/16; accepted 03/15/16. Author for correspondence: Jui-Ching Chou (e-mail: dglin@dragon.nchu.edu.tw).
[1] *Department of Soil and Water conservation, National Chung-Hsing University, Taichung, Taiwan, R.O.C.*
[2] *Department of Civil Engineering, Kao-Yuan University, Kaohsiung, Taiwan, R.O.C.*
[3] *Sinotech Engineering Consultants, Taipei, Taiwan, R.O.C.*

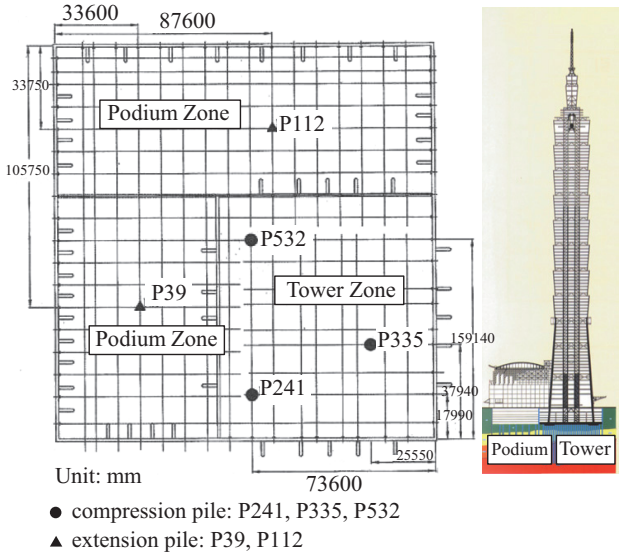

Fig. 1. Plan view of excavation zone and location of testing piles.

Table 1. Input model parameters of soil layers and the pile.

Depth Soil layer	c' (kPa)	ϕ' (°)	ν'	E' (MPa)	γ_d (kN/m^3)	ψ (°)
0~2 m Surfce fill	2.0	30.0	0.3	9.4	13.0	0.0
2~23 m Silty clay 1	5.0	28.0	0.3	12.6	13.1	0.0
23~32 m Silty clay 2	10.0	30.0	0.3	14.4	13.1	0.0
32~41 m Silty sand	20.0	32.0	0.3	19.2	15.5	0.0
41~50 m Silty gravel	0.0	35.0	0.3	22.8	15.7	2.0
50~86 m Sandstone	100.0	45.0	0.3	111.0	18.8	3.0
Test Pile	Pile diameter = 1.5 m, Pile length = 72 m ν = 0.23, E = 33500 MPa, γ_d = 23.5 kN/m^3					

Table 2. Parameters of interface elements.

Pile Depth	k_s (MPa)	k_n (MPa)	c_s (kPa)	c_n (kPa)	ϕ_s (°)	ϕ_n (°)
0~2 m	93.6	4.5	1.3	1.8	21.0	20.0
2~23 m	94.0	6.3	3.3	4.4	19.5	19.0
23~32 m	95.0	7.2	6.7	8.9	21.0	20.0
32~41 m	110.0	14.4	13.3	17.7	22.6	22.0
41~50 m	130.0	45.7	0.0	0.0	25.0	24.0
50~80 m	212.0	55.4	66.6	88.5	33.6	33.0

* k_s = (4.9~25.8) × G, k_n = (0.478~2) × E, c_s = (2/3)×c', c_n = 0.9×c' and $\phi_s = \tan^{-1}[(2/3) \times \tan\phi']$, $\phi_n = \tan^{-1}[(2/3) \times \tan\phi']$

were instrumented with strain gauges and rebar transducers to estimate the load distribution and deformation. In this article, comparisons between pile loading tests and numerical simulations for compression pile P241 and extension pile P112 are presented. The extension loading test of P39 was performed from April 19 to 21, 1999, with the maximum load of 20 MN (= 2041 Ton) and the compression loading test of P241 loading test was performed from March 12 to 14, 1999, with the maximum load of 29.4 MN (3000 Ton). The ASTM D3689-83 and ASTM D1143-81 were followed for the loading procedures of extension and compression loading tests respectively.

In the pile loading test simulation, the soil mass was modeled by soil block elements and the pile was modeled by pile structure elements with interface elements. Soil parameters for numerical analyses on *Taipei 101* field site were determined by Lin and Woo (2000, 2005) based on 128 boring logs with high quality field tests and laboratory tests. The ground water table was set at 2 m below the ground surface. Soil was modeled using Mohr-Coulomb (M-C) model and the pile was simulated using Linear Elastic (L-E) model. During pile loading tests, the loading was applied in a small increment and maintained at least for 2 hrs or for a settlement rate of pile head lower than 0.25 mm/hr to ensure the dissipation of pore water pressure. As a result, the simulation of pile loading tests was carried out by effective and drained analyses. Input model parameters of soil and pile are listed in Table 1 including cohesion (c'), friction angle (ϕ'), Poisson ratio (ν'), Young's modulus (E'), dry unit weight (γ_d) and dilation angle (ψ).

Interface elements simulate the normal and shear direction interactions of pile shaft with surrounding soil mass via shear coupling spring and normal coupling spring. Parameters of coupling spring are cohesion (c_s & c_n), friction (ϕ_s & ϕ_n) and spring stiffness (k_s & k_n). Subscript-s is for shear coupling spring and subscript-n is for normal coupling spring. In this study, the interface parameters are adjusted based on Desai et al. (1984) to model the pile loading test. Then, the comparisons of load transfer and settlement curves between simulation and observation are made to obtain a set of values which can give the best curve fitting. The interface parameters are listed in Table 2.

Fig. 2 shows the load-settlement curves at the pile top, the level of the basement and the pile tip. Results of numerical predictions and measurements of the compression pile (P241) are in a good agreement. Only at the final loading increment, the numerical simulation underestimates about 10% at the pile head and 25% at the pile tip. Results of numerical predictions of the extension pile are deviated from the measured settlement. The settlement at the final loading stage is underestimated 53% at the pile head and 46% at the excavation level. This deviation may be caused by the extension type of loading, especially in a high loading level, which is different from the compressive loading considered in the soil model.

Figs. 3 and 4 present the load transfer curves under various loading levels. For the compression pile loading test (P_{dc} = design load = 12,000 kN), predictions and measurements are almost identical at lower loading level (1.1 P_{dc} and 0.55 P_{dc}). For the extension pile loading test (P_{de} = design load=10,000 kN), predictions and measurements are similar for a wide

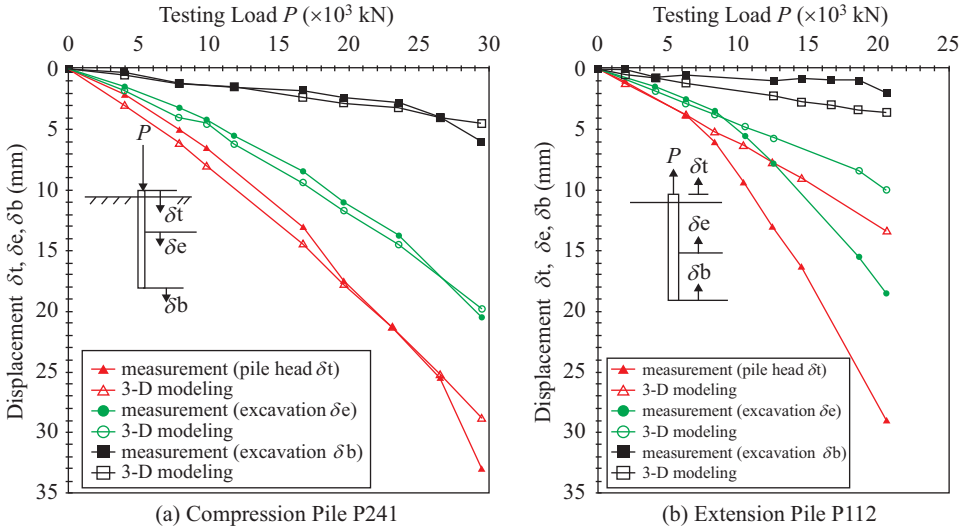

Fig. 2. Load-settlement curves of at different elevations.

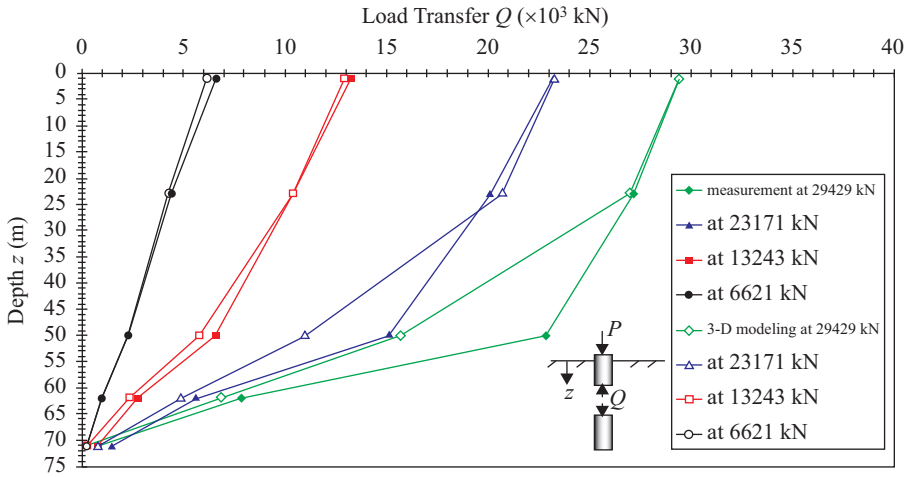

Fig. 3. Load transfer curves of compression pile P241 at different loading levels.

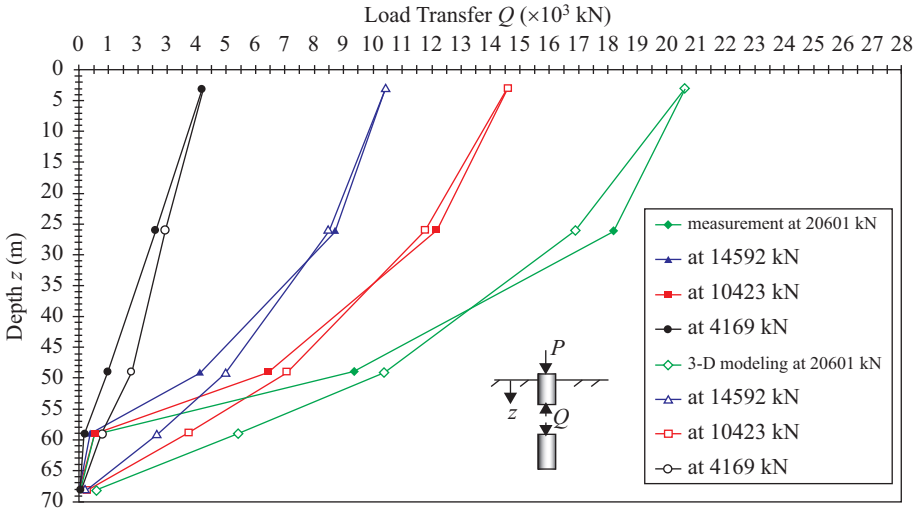

Fig. 4. Load transfer curves of extension pile P112 at different loading levels.

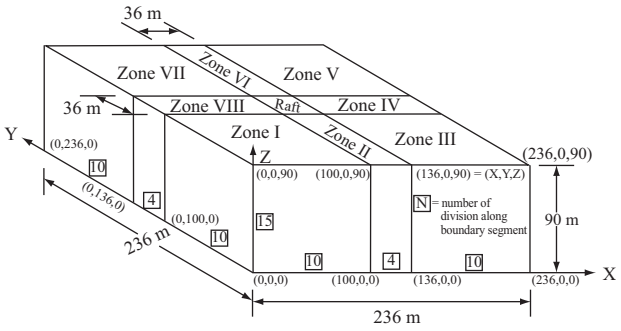

Fig. 5. Different zones for element size consideration.

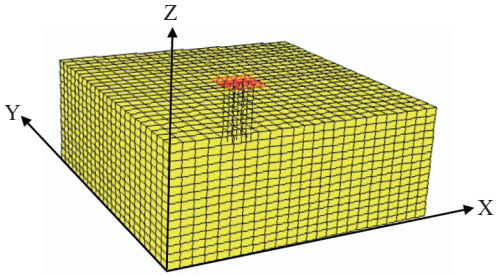

(a) Finite difference discretization of piled-raft foundation

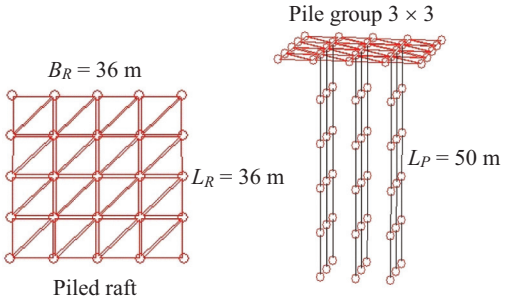

(b) Raft slab (c) Piled-raft with pile group

Fig. 6. Detailed FLAC 3D grid.

range of loading level (2.06~0.42 P_{de}). However, the numerical modeling underestimates in the compression pile loading test and overestimates in the extension pile test at the depth of 50 m (Sand Stone stratum). This deviation may be resulted from the generalized soil profile adopted for numerical simulations in Sand Stone stratum.

Overall, FLAC 3D analyses can capture the deformation behavior of the pile fairly well. Therefore, above simulation procedures and parameters are considered justified and valid to use in the following parametric study.

III. PARAMETRIC STUDY

1. Numerical Model

The geometry model used in the parametric study is shown in Fig. 5. The model consists of nine zone blocks (Zone I~VIII and Zone Raft) with an area of 236 m × 236 m × 90 m. Fig. 6

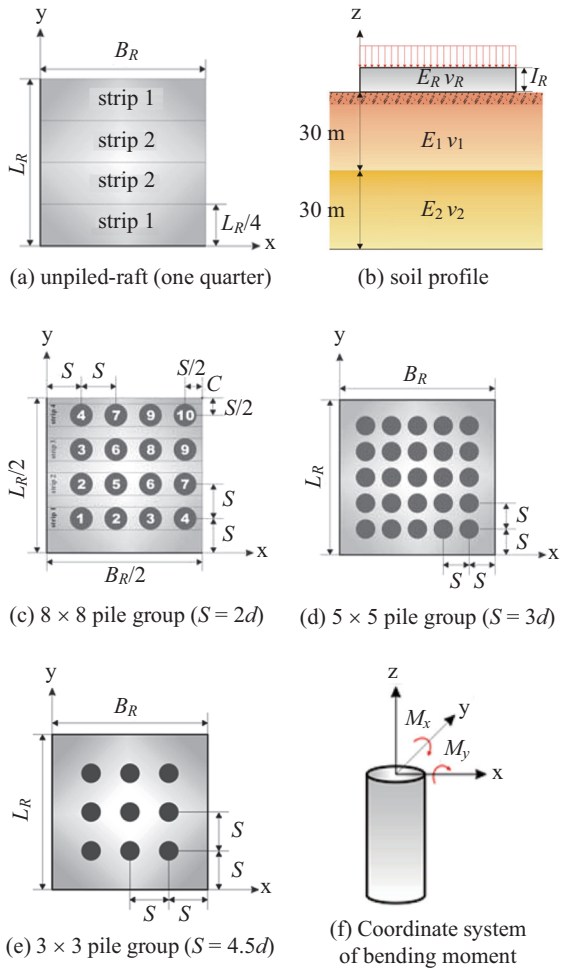

(a) unpiled-raft (one quarter) (b) soil profile

(c) 8 × 8 pile group ($S = 2d$) (d) 5 × 5 pile group ($S = 3d$)

(e) 3 × 3 pile group ($S = 4.5d$) (f) Coordinate system of bending moment

Fig. 7. Pile configurations.

shows the details of 3-D finite difference grid of the piled-raft foundation with 3 × 3 pile group.

An unpiled-raft and three piled-raft foundations with identical raft dimension of $L_R \times B_R$ = 36 m × 36 m and various raft thickness (t_R = 1 m, 2 m and 3 m) and various pile configurations were analyzed. The pile configurations are shown in Fig. 7 including 8 × 8 (pile spacing $S = 2 \times d = 4$ m), 5 × 5 ($S = 3 \times d = 6$ m) and 3 × 3 ($S = 4.5 \times d = 9$ m) pile group with pile diameter d = 2 m, pile length L_p = 50 m.

In the parametric study, the soil mass and the pile were modeled followed the pile loading test simulation. The raft slab of the piled-raft foundation was modeled by shell structure elements with a linearly elastic material and no failure limit. Input parameters of the raft are the same as the pile. In addition, an idealized Taipei Metropolitan soil profile was used for analyses. Input model properties are listed in Tables 2 and 3.

2. Settlement of Piled Raft

Fig. 8 shows vertical displacement contours of the piled-raft with 8 × 8 pile group and the unpiled-raft under a uniform loading of 1000 kPa. Both rafts deform in a bowl shaped settlement pattern same as observations from Poulos et al. (1997);

Table 3. Input parameters of soil layers and the piled-raft foundation.

Depth Soil layer	c'(kPa)	ϕ'(°)	ν'	E'(MPa)	γ_d(kN/m^3)	ψ(°)
0~30 m Silty clay	2.0	30.0	0.3	9.4	13.0	0.0
30~60 m Sandstone	5.0	45.0	0.3	12.6	13.1	0.0
Raft	Thickness 1 m, 2 m and 3 m; ν = 0.16, E = 33500 MPa, γ_d = 23.5 kN/m^3					
Pile	Diameter = 2 m Length = 50 m; ν = 0.16, E = 33500 MPa, γ_d = 23.5 kN/m^3					

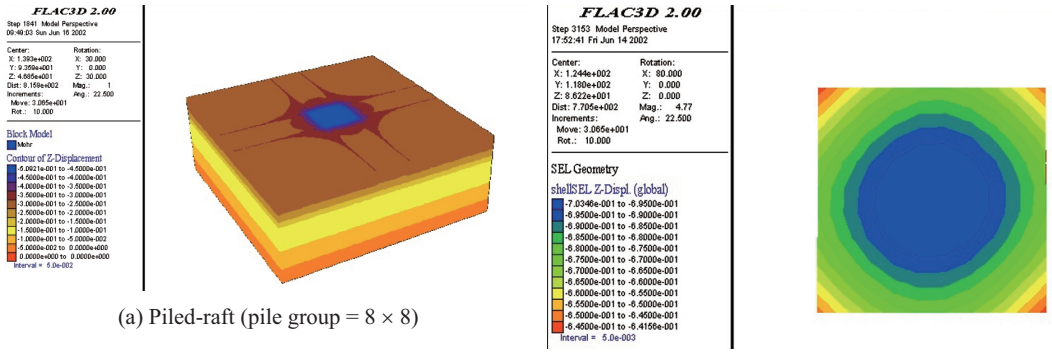

(a) Piled-raft (pile group = 8 × 8)

(b) Unpiled-raft

Fig. 8. Vertical displacement contours under loading of 1000 kPa.

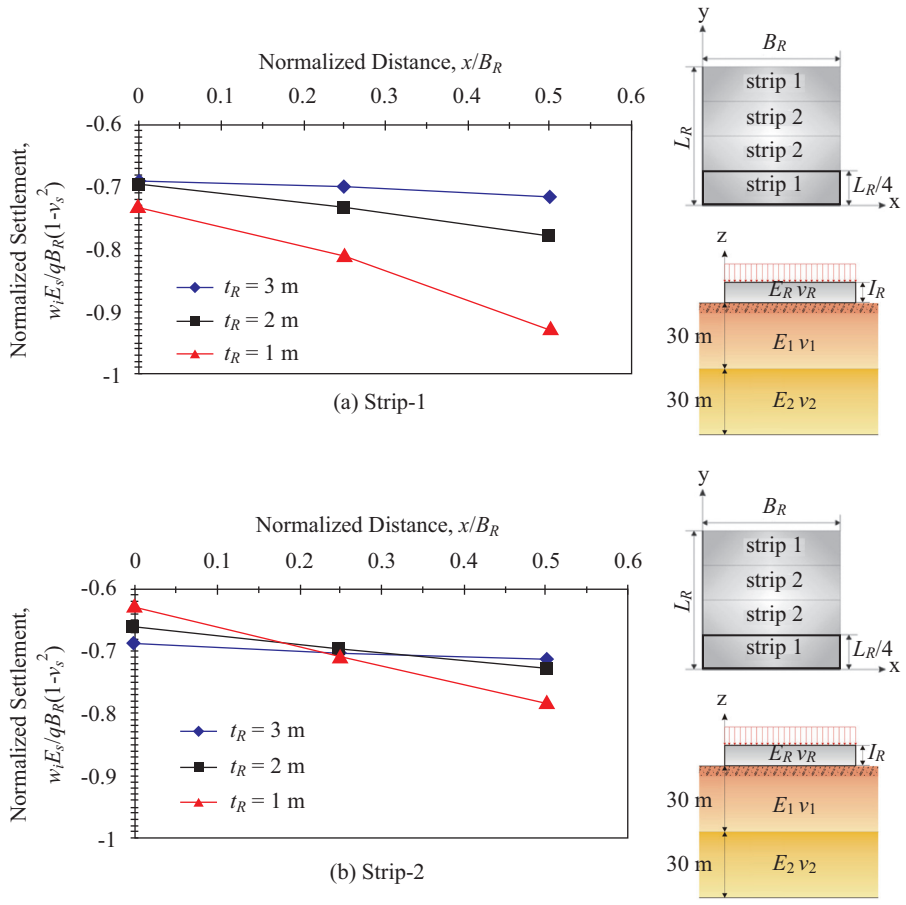

(a) Strip-1

(b) Strip-2

Fig. 9. Normalized settlement of unpiled-raft at loading of 1000 kPa.

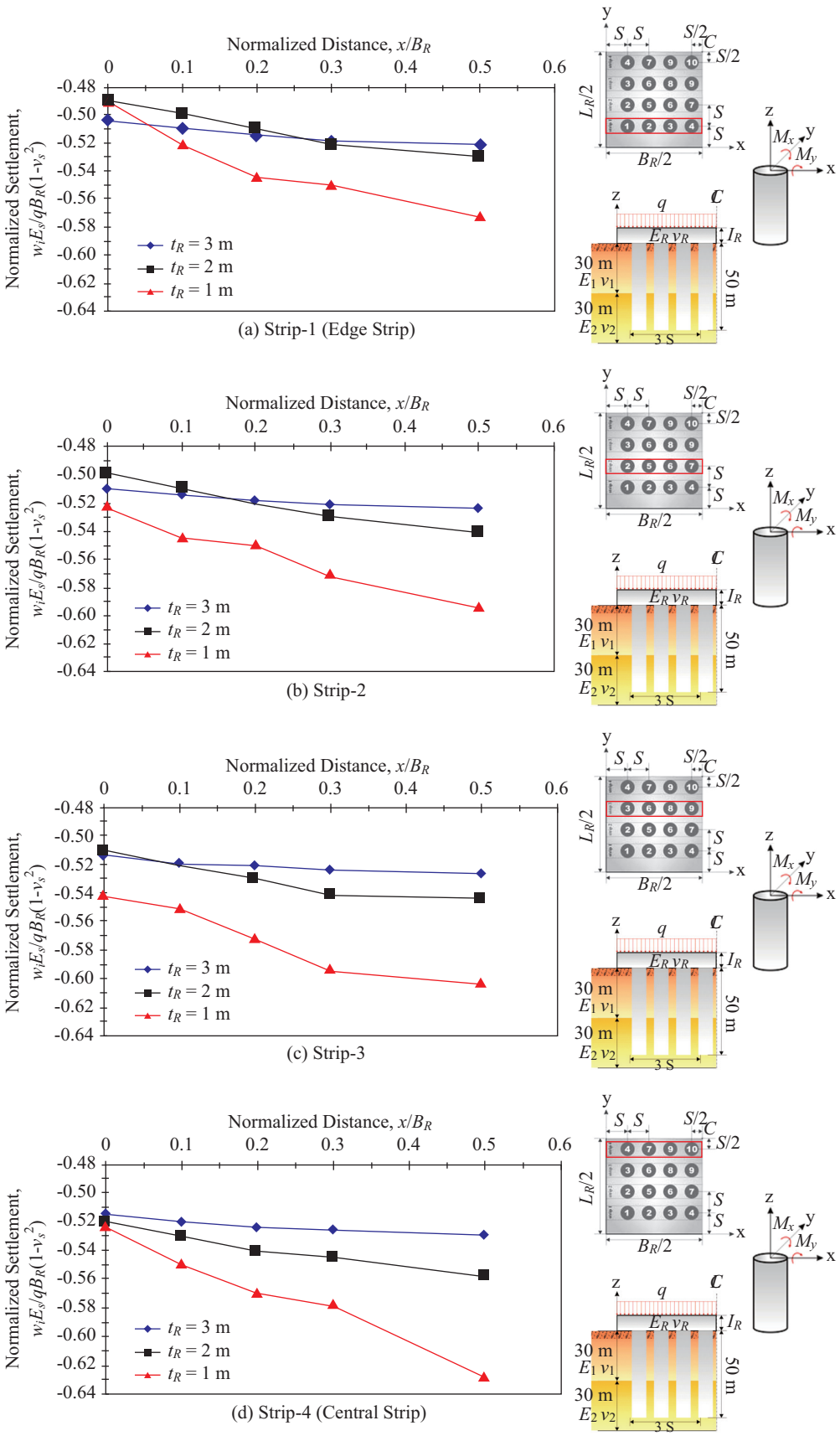

Fig. 10. Normalized settlement of piled-raft (8 × 8, $S = 2d$) at loading of 1000 kPa.

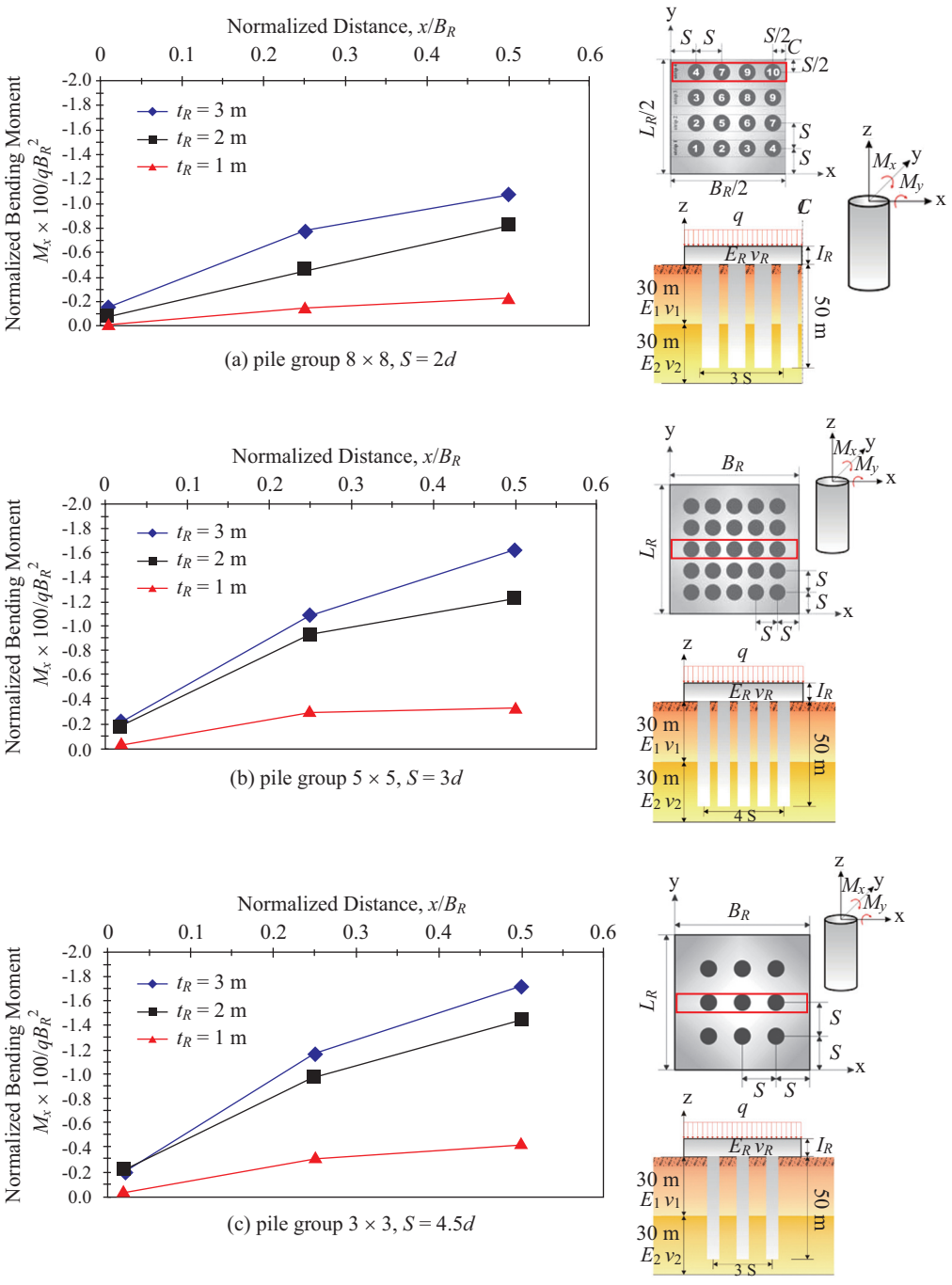

Fig. 11. Normalized bending moment of central strip of piled-raft at loading of 1000 kPa.

Comodromos et al. (2009); Lee et al. (2010) and Poulos et al. (2011).

Figs. 9 and 10 show the normalized settlement of the unpiled-raft and the piled-raft with 8 × 8 pile group at different raft locations. The normalized settlement is defined as $(w_i \times E_s)/(q \times B_R \times (1-\nu_s^2))$ where w_i is the settlement of the raft, E_s is the Young's modulus of the soil, q is the applied load and ν_s is Poisson ratio of soil. Results show that piles can effectively reduce the average and maximum settlements of the raft. Maximum settlements in center strip (*strip-4*) of the piled-raft (raft thickness 1 m to 3 m) are reduced by 32.3%, 28.5% and 26.2% respectively comparing to the center strip (*strip-2*) of the unpiled-raft. Same observations were found in previous studies (Long, 2010; Karim et al., 2013; Nguyen et al., 2013). Meanwhile, it is found that the differential settlement reduces as the raft thickness increases. The maximum differential settlement of the center strip of the raft is reduced about 50%. The same trend is also shown by several researches (Oh et al., 2009;

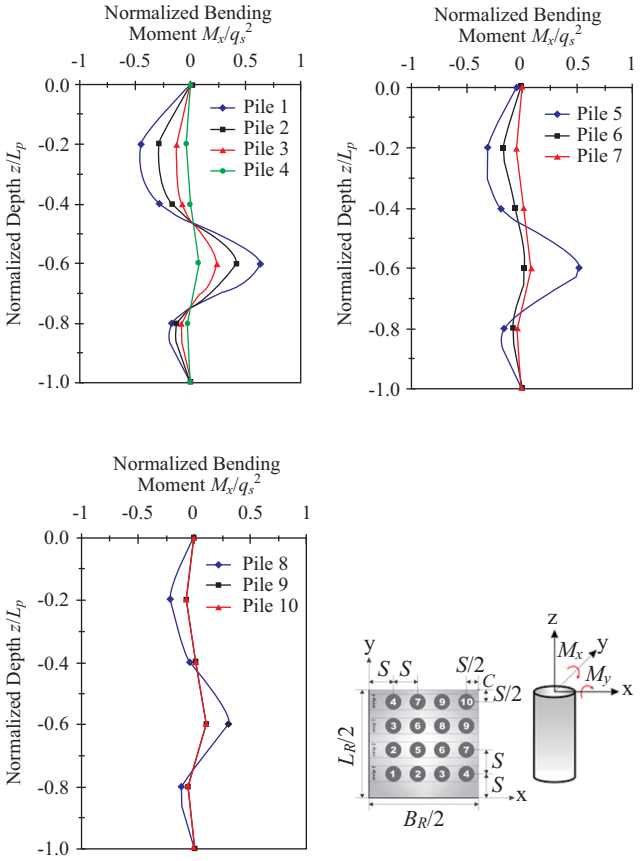

Fig. 12. Normalized bending moment of central strip of piled-raft at loading of 1000 kPa.

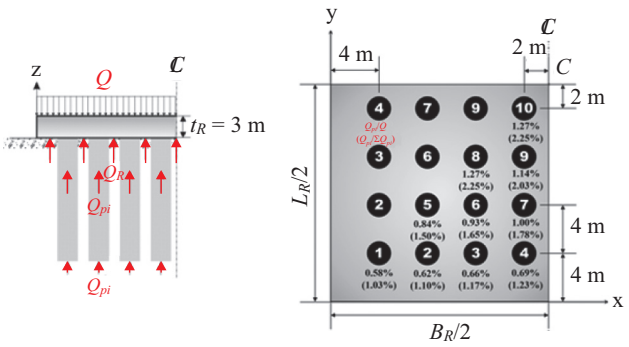

Fig. 13. Load carrying ratio of piles at loading 1000 kPa (8 × 8 pile group, $S = 2d$, $d = 2$ m, $B_R \times L_R = 36$ m × 36 m, $t_R = 3$ m).

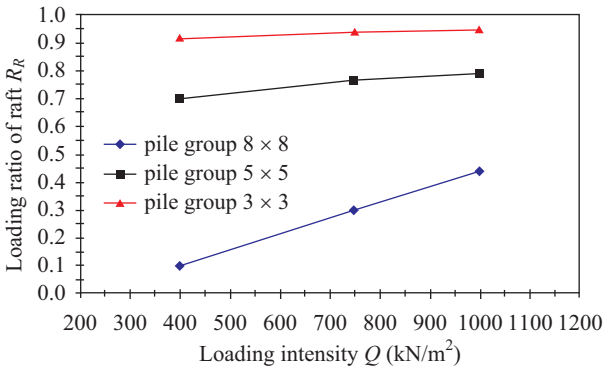

Fig. 14. Load carrying ratio of piled-raft for various loading intensity ($t_R = 3$ m).

Rabiei, 2009; El-Garhy, 2013).

3. Bending Moment of Piled Raft

For all pile configurations (8 × 8, 5 × 5 and 3 × 3), the bending moment (M_x) of the raft increases with the increase of the raft thickness as shown in Fig. 11. For the same raft thickness, the bending moment of the piled-raft decreases with the increase of the pile number. For the raft thickness of 3 m, the maximum normalized bending moments ($M_x \times 100/qB_R^2$) are 1.08, 1.63 and 1.71 for 8 × 8, 5 × 5 and 3 × 3 pile group respectively. As compared with those developed in the unpiled-raft (1.52), only the case of the piled-raft with 8 × 8 pile group reduces the raft bending moment effectively.

Fig. 12 presents the normalized bending moment distribution along the pile shaft under loading intensity of 1000 kPa (pile group 8 × 8, $S = 2d$) acting on the piled-raft. The bending moment of the piles is affected by the settlement pattern of the raft. Because of the symmetric settlement pattern, the inner piles experience less horizontal movements. Therefore, the bending moments on the inner piles (Pile 8, 9 and 10) are less than on the outer piles (Pile 1, 2 and 5). For a single pile, the maximum bending moment occurs at the interface of the silty clay layer and sand stone bearing layer (GL -30 m = Normalized Depth 0.6). It can be inferred that the pile segment at the transition zone from the soft soil layer to the stiff bearing layer may carry a higher bending moment.

4. Load-Carrying Ratio of Piled Raft

Fig. 13 illustrates the loading mechanism of the piled-raft system and the loading distribution percentage carried by piles. A load carrying ratio of piled-raft $R_R (= Q_R/Q = (Q - \Sigma Q_{pi})/Q)$ is introduced and calculated as shown in Fig. 14. In which, (Q) is the total loading carried by the piled-raft system whereas (ΣQ_{Pi}) and (Q_R) represent the loading portions carried by piles and the raft respectively.

Meanwhile, Fig. 13 also reveals that piles near the raft center carry a higher percentage of loading than those adjacent to the raft edge. However, pile load measurements of the Messe-Torhaus in Frankfurt presented in Small and Poulos (2007) and numerical simulation results in Bourgeois et al. (2012) show central piles carrying a smaller loading than corner piles. One possible reason of this discrepancy could be the raft area which piles share the loading with. In this article, the distance from the edge of the raft to the center of the corner is 2d and that distance in Small and Poulos (2007) and Bourgeois et al. (2012) is 1d. Therefore, the raft area shares the loading for corner piles (Pile 1 to 4) is 6 m × 6 m. Other piles (Pile 5 to 10) only have a raft area of 4 m × 4 m sharing the loading. This area difference causes corner piles carrying a smaller loading

than central piles.

As shown in Fig. 14, for pile group 8 × 8, the raft shares 43.8% (= $R_R = Q_R/Q$) of the total vertical load (Q) for the loading intensity of 1,000 kPa while it appears 30.2%, 10% of total vertical load for 750 and 400 kN/m^2 with the raft thickness of 3 m. R_R increases as the loading increases and the number of piles decreases. From previous studies, the load carrying ratio of piled-raft varies from 15% to 70% depending on many factors such as the raft thickness, number of piles, pile length, configuration of piles, soil profile and loading level (Liang et al., 2003; Lee et al., 2010; El-Garhy et al., 2013). Centrifuge test results of Lee et al. (2010) show that R_R increases as the settlement of the piled-raft increases (loading increases) or as the number of piles decreases. R_R trends in this study agree with above observations.

IV. CONCLUSIONS

The piled-raft system is commonly used as the foundation of the high-rise building. The conventional design of the piled-raft foundation in Taiwan usually ignores the contribution of the load carrying by the raft. It makes engineers overdesign in the piled-raft foundation. This article attempts to understand the complex interaction between the piles, raft and soil via a pile load test simulation and a parametric study using FLAC 3D.

The pile load test simulation analyzed pile load tests from *Taipei 101* Construction Project. In the simulation, soil layers were modeled using the *M-C* soil model and the pile was modeled using pile structure elements with interface elements. Simulation results indicate that FLAC 3D can capture the deformation behavior of the pile fairly well.

The parametric study was performed using FLAC 3D with the same procedures of the pile load test simulation and the idealized typical Taipei Metropolitan soil profile. Parametric study results show: (1) the piled-raft foundation reduces the settlement and the differential settlement of the raft; (2) the thicker raft reduces the settlement and the differential settlement of the raft; (3) only the case of the piled-raft with 8 × 8 pile group reduces the raft bending moment; and (4) the raft can carry a higher percentage of loading when the loading increases and the number of piles decreases.

Observations from the parametric study indicate that ignoring the bearing capacity contribution of the raft results in overdesign in the conventional foundation design practice. In addition, assuming piles carrying the same loading in the conventional foundation design practice is not true either. In the future piled-raft foundation project, it is recommended to use 3D numerical simulation help engineers understand the loading distribution mechanisms and optimize the foundation design.

REFERENCES

Bourgeois, E., P. De Buhan and G. Hassen (2012). Settlement analysis of piled-raft foundations by means of a multiphase model accounting for soil-pile interactions. Computers and Geotechnics 46, 26-38.

Clancy, P. and M. F. Randolf (1993). An approximate analysis procedure for piled raft foundations. International journal for numerical methods in geomechanics 17, 849-869.

Comodromos, E. M., M. C. Papadopoulou and I. K. Rentzeperis (2009). Pile foundation analysis and design using experimental data and 3-D numerical analysis. Computers and Geotechnics 36(5), 819-836.

Desai, C. S., M. M. Zaman, J. G. Lightner and J. J. Siriwardanej (1984). Thin-layer element for interfaces and joints. Int. J. for Numer. and Analyt. Methods in Goemech 8, 19-43.

El-Garhy, B., A. A. Galil, A. F. Youssef and M. A. Raia (2013). Behavior of raft on settlement reducing piles: Experimental model study. Journal of Rock Mechanics and Geotechnical Engineering 5(5), 389-399.

Karim, H. H., M. R. AL-Qaissy and M. K. Hameedi (2013). Numerical analysis of piled raft foundation on clayey soil. Eng. & Tech. Journal 31(7) Part (A), 1297-1312.

Lee, S. W., W. W. L. Cheang, W. M. Swolfs and R. B. J. Brinkgreve (2010). Modelling of piled rafts with different pile models. Proceedings of the 7th European Conference on Numerical Methods in Geotechnical Engineering. Trondheim, Norway: CRC Press, 637-642.

Liang, F. Y., L. Z. Chen and X. G. Shi (2003). Numerical analysis of composite piled raft with cushion subjected to vertical load. Computers and Geotechnics 30(6), 443-453.

Lin, D. G. and S. M. Woo (2000). Deformation analysis of Taipei International Financial Center deep excavation project, technical report. Trinity Foundation Engineering Consultants Co., LTD.

Lin, D. G. and S. M. Woo (2005). Geotechnical analyses of Taipei International Financial Center (*Taipei 101*) Construction Project, 16th International Conference on Soil Mechanics and Geotechnical Engineering, 1513-1516, September 12-16, 2005, Osaka, Japan.

Long, P. D. (2010). Piled raft - a cost-effective foundation method for high-rises. Geotechnical Engineering 41(3), 1-12.

Nguyen, D. D. C., S. B. Jo and D. S. Kim (2013). Design method of piled-raft foundations under vertical load considering interaction effects. Computers and Geotechnics 47, 16-27.

Nguyen, D. D. C., D. S. Kim and S. B. Jo (2014). Parametric study for optimal design of large piled raft foundations on sand. Computers and Geotechnics 55, 14-26.

Oh, E. Y. N., Q. M. Bui, C. Surarak and A. S. Balasurbamaniam (2009). Investigation of the Behavior of Piled Raft Foundations in Sand by Numerical Modeling. In The Nineteenth International Offshore and Polar Engineering Conference. International Society of Offshore and Polar Engineers.

Poulos, H. G. (1991). Analysis of piled strip foundations. Computer methods and advances in geomechanics (1), 183-191.

Poulos, H. G. (1994). An approximate numerical analysis of pile-raft interaction. International Journal for Numerical and Analytical Methods in Geomechanics 18(2), 73-92.

Poulos, H. G. and E. H. Davis (1980). Pile foundation analysis and design. John Wiley and sons, New York.

Poulos, H. G., J. C. Small and H. Chow (2011). Piled raft foundations for tall buildings. Geotechnical Engineering Journal of the SEAGS and AGSSEA 42(2), 78-84

Poulos, H. G., J. C. Small, L. D. Ta, J. Sinha and L. Chen (1997). Comparison of some methods for analysis of piled rafts. Proceedings of the 30th year symposium of the Southeast Asian Geotechnical Society 5, 1-6.

Rabiei, M. (2009). Parametric Study for Piled Raft Foundations. EJGE 14.

Randolph, M. F. (1983). Design of piled raft foundations. Cambridge University Engineering Department.

Randolph, M. F., R. Dolwin and R. Beck (1994). Design of driven piles in sand. Geotechnique 44(3), 427-448.

Small, J. C. and H. G. Poulos (2007). Nonlinear analysis of piled raft foundations. Geotechnical Special Publication GSP158, ASCE, CD Volume, GeoDenver, 1-9.